NIH Public Access
Author Manuscript
Sci Signal. Author manuscript; available in PMC 2013 December 31.

Published in final edited form as:
Sci Signal. ; 5(251): . doi:10.1126/scisignal.2003431.

Sumoylation Silences Heterodimeric TASK Potassium Channels Containing K2P1 Subunits in Cerebellar Granule Neurons

Leigh D. Plant, **Leandro Zuniga**, **Dan Araki**, **Jeremy D. Marks**[1], and **Steve A. N. Goldstein**[2]
Department of Biochemistry, Brandeis University, 415 South Street, Waltham MA 02454

[1]Department of Pediatrics and Institute for Molecular Pediatrics Sciences, Pritzker School of Medicine, University of Chicago, 5271 S. Maryland Avenue, Chicago, IL 60637 USA

Abstract

The standing outward K^+ current (IKso) governs the response of cerebellar granule neurons to natural and medicinal stimuli including volatile anesthetics. In this study, we showed that sumoylation silenced half of IKso at the surface of cerebellar granule neurons because the underlying channels were heterodimeric assemblies of K2P1, a subunit subject to sumoylation, and the two P domain, acid-sensitive K^+ (TASK) channel subunits, K2P3 or K2P9. The heteromeric channels comprised the acid-sensitive portion of IKso and mediated its response to halothane. We anticipate that sumoylation also influences sensation and homeostatic mechanisms in mammals through TASK channels formed with K2P1.

INTRODUCTION

The importance of background (leak) potassium currents to excitable membrane function has been appreciated since the 1940s (1, 2). Regulated by numerous stimuli (3), leak currents are passed by K2P channels (4). Identified by a unique primary structure of two pore-forming (P) domains in each subunit, K2P channels operate as classical, potassium-selective open rectifiers (5–9) and stabilize the resting membrane potential of excitable cells below the threshold for firing action potentials. Encoded by 15 *KCNK* genes in humans, two K2P subunits assemble to create a single ion conduction pathway (10–14). Here, we reveal a mechanism of K2P regulation in cerebellar granule neurons that is expected to have broad biological implications because K2P3 and K2P9 are emerging as central to the biology of blood pressure, nociception, olfaction and oxygen sensation, K2P1 is present along with K2P3 or K2P9 in the tissues controlling these processes, and SUMO is present in all cells.

TASK channels are homodimeric and heterodimeric complexes of K2P3 and K2P9 subunits (15) that are blocked by protonation of a His residue in the first P domain of each subunit in the physiological pH range (10, 16, 17). The subunits share overlapping distributions in the central and peripheral nervous systems (18, 19), the carotid body (20), the heart and cardiopulmonary circulation (16, 21, 22), the adrenal cortex (23, 24) and T lymphocytes (25). In cerebellar granule neurons, K2P3 and K2P9 subunits have been proposed to underlie the acid-sensitive portion of the standing outward potassium current, IKso, and thereby to mediate neuronal responses to pH (26), pO_2 (27), neurotransmitters (26, 28), pungent flavors (29), and volatile anesthetics, including halothane (30).

[2]Address correspondence to: goldstein@brandeis.edu.

Author contributions: L.D.P. and J.D.M. designed and performed experiments, analyzed data and wrote the manuscript. L.Z. and D.A. performed experiments. S.A.N.G. conceived and designed experiments and wrote the manuscript. Competing interests: The authors declare that they have no competing interests.

NIH-PA Author Manuscript
NIH-PA Author Manuscript
NIH-PA Author Manuscript

NIH-PA Author Manuscript

NIH-PA Author Manuscript

NIH-PA Author Manuscript

This study was launched by our observations that application of the desumoylase SENP1 rapidly increases IKso in rat cerebellar granule neurons, suggesting that the endogenous SUMO pathway inhibits IKso, and that channels formed exclusively by K2P3 or K2P9 are insensitive to regulation by sumoylation. This led us to suspect that IKso channels incorporated K2P1 for the following reasons. K2P1 is present along with K2P3 and K2P9 in the granule cell layer of cerebellum (18, 31). K2P1 channels are silent at the cell surface (32) due to sumoylation of Lys^{274}. Desumoylation activates K2P1 channels to reveal a potassium-selective leak current that is acid-sensitive by the same His-dependent mechanism as K2P3 and K2P9 (12, 33). Finally, one SUMO monomer is conjugated to one K2P1 subunit and this is necessary and sufficient to silence a dimeric channel (12).

Here, we demonstrated the presence of mRNAs encoding K2P1, K2P3 and K2P9 in individual cerebellar granule neurons using single-cell, single-transcript analysis. K2P1 subunits assembled with K2P3 or K2P9 in live mammalian cells using Förster resonance energy transfer (FRET) and complexes were detergent-stable. K2P1 formed functional channels with K2P3 or K2P9 and thereby conferred regulation by SUMO. Single-particle fluorescent microscopy showed that each K2P1 subunit provided a single SUMO conjugation site and that one SUMO moiety silenced mixed subunit channels. In cerebellar granule neurons, ~50% of IKso channels at the cell surface were held silent by sumoylation. Release from suppression by desumoylation revealed that at least 80% of total IKso was indeed carried by K2P channels. Halothane augmented IKso 100% when channels with K2P1 were silenced by SUMO. Upon desumoylation, halothane augmented IKso 300%. The findings indicate that the acid-sensitive portion of IKso is the same as both the SUMO-sensitive part of the current and the halothane responsive component.

RESULTS

KCNK1, KCNK3 and *KCNK9* transcripts are present in single cerebellar granule neurons

In situ hybridization studies of rat (19) and mouse (31) cerebellum demonstrated transcripts for *KCNK1*, *KCNK3* and *KCNK9* (which encode K2P1, K2P3 and K2P9 subunits, respectively) in the granule cell layer. To determine if the three genes were expressed together in the same cells, we developed a method employing confocal microscopy, custom-designed, mRNA-specific probes, and cyanine dye-based signal amplification to simultaneously identify *KCNK1*, *KCNK3* and *KCNK9* transcripts in individual rat cerebellar granule neurons in primary culture. Thin confocal sections extending from the cover slip to the top of the cells were obtained at maximum resolution and 3D reconstructions were generated (Fig. S1A, Movie S1). Fluorescent particles corresponding to *KCNK1*, *KCNK3* and *KCNK9* transcripts were present in all neurons studied (Fig. S1B). Although particle size correlated with fluorescent intensity ($r > 0.98$), size distribution differed for the three probes making it uncertain if particles represented one or multiple transcripts (Fig S1C–E). Mean relative particle densities for *KCNK1*, *KCNK3* and *KCNK9* were 2:8:1.

Native K2P1 and SUMO1 interact at the surface of cerebellar granule neurons

Seeking evidence for close association of SUMO1 and K2P1 at the surface of rat cerebellar granule neurons we employed antibody-mediated FRET, a method we have previously used with cultured hippocampal neurons (34). FRET occurs over short distances (1–10 nm) and is therefore indicative of close association. We localized SUMO1 and K2P1 with validated primary antibodies (Figure S2) and visualized the proteins with fluorophores on secondary antibodies. We observed FRET between SUMO1 and K2P1 (that is, increased donor fluorescence intensity on photobleaching of the acceptor fluorophore) and thus demonstrated proximity between these proteins (Figure 1, K2P1). In contrast, the *KCNK2* gene product K2P2 (also called TREK1) was present in cerebellar granule neurons, but failed to exhibit

NIH-PA Author Manuscript

NIH-PA Author Manuscript

NIH-PA Author Manuscript

FRET with SUMO1 (Figure 1, K2P2). These findings indicate close association of SUMO1 with K2P1 but not with K2P2.

Unexpectedly, native K2P3 and K2P9 also exhibited FRET with SUMO1 in cerebellar granule neurons (Figure 1). This was surprising because the residue in K2P1 that is sumoylated, Lys^{274}, is not present in K2P2, K2P3 or K2P9. This suggested either that a lysine residue in K2P3 and K2P9 was subject to sumoylation or that mixed assemblies with K2P1 carried SUMO1 into the channels. To validate this finding we studied interactions between heterologously-expressed K2P9 and native SUMO1 in Chinese hamster ovary (CHO) and confirmed that FRET was only observed when K2P1 was also expressed (Figure S3). Therefore, we compared the consequences of SUMO on IKso and cloned K2P channels.

SENP1 activates IKso and K2P1 channels but not K2P2, K2P3 or K2P9 channels

The observation that SUMO regulates IKso in rat cerebellar granule neurons was made using established recording protocols to assess the current (27, 35) and various pH levels that encompassed the range over which IKso (26) and channels formed by K2P1, K2P3 and K2P9 show acid-sensitivity (10, 12, 16, 17, 33). We assessed IKso, resting membrane potential (Vm) and input resistance (R_{IN}), a measure of cellular excitability determined by the number of open channels. In keeping with prior studies, external acidification markedly decreased IKso, thereby increasing membrane resistance and depolarizing the resting membrane potential, resulting in increased neuronal excitability. Similarly, external alkalinization increased IKso, thereby decreasing membrane resistance and hyperpolarizing the resting membrane potential, resulting in decreased neuronal excitability. The magnitude of IKso (pA/pF) was ~250 at baseline (pH 7.4), ~125 at pH 6.4 and ~300 at pH 8.4 (Figure 2A, Table S1).

To study the effects of sumoylation and desumoylation, we included purified SUMO1 or SENP1 proteins in the patch pipettes at picomolar concentrations previously shown to produce maximal effects on human K2P1 channels expressed in CHO cells (12) and on cloned and native Kv2.1 channels in hippocampal neurons (34). Addition of SUMO1 did not alter the magnitude of IKso, Vm, R_{IN} or sensitivity of these parameters to pH consistent with sumoylation of membrane potassium channels at baseline (Figure 2A). In contrast, application of the desumoylase SENP1 decreased excitability by doubling IKso, thereby shifting Vm toward E_K and lowering R_{IN} (Figure 2A, Table S1). These changes were augmented at pH 8.4 and absent at pH 6.4, consistent with action of the SUMO pathway on pH-dependent currents.

To assess the effect of sumoylation and desumoylation on K2P1, K2P3 and K2P9, we expressed the subunits individually in CHO cells and studied them in excised membrane patches. As previously reported (12), K2P1 is sumoylated at rest by endogenous SUMO pathway enzymes. Thus, membrane patches excised from CHO cells expressing K2P1 were electrically quiet (12 ± 5 pA at 50 mV) until SENP1 was applied and the current increased to 385 ± 22 pA; subsequent application of SUMO1 suppressed the current back to baseline levels (Figure 2B). Sumoylation is reversible, and re-exposure to SENP1 released K2P1 channels from inhibition by SUMO and activity was maintained after the enzyme was washed away (Figure 2B). In contrast, homomeric K2P2, K2P3 and K2P9 channels were active in excised patches at baseline and passed robust currents that were insensitive to application of either SUMO1 or SENP1 (Figure 2C). These observations suggested that FRET between native SUMO1 and K2P3 or K2P9 in cerebellar granule neurons was observed due to co-assembly with K2P1. Accordingly, we sought direct evidence for heteromeric subunit association.

NIH-PA Author Manuscript

NIH-PA Author Manuscript

NIH-PA Author Manuscript

K2P1 shows FRET with K2P3 and K2P9 but not K2P2 in live CHO cells

To directly assess the assembly of K2P subunits at the surface of living cells, we measured FRET between subunits using donor photobleaching (12, 34). K2P1 subunits were tagged with yellow or cyan fluorescent protein (YFP or CFP) at the N-terminus, a site that tolerates insertion of fluorescent proteins (33). Both YFP and CFP tagged K2P1 subunits reached the surface when they were co-expressed (Figure 3A and S4A). The time course of CFP decay under continuous illumination (as assessed by the time constant τ for donor photobleaching) was then measured. The τ for the decay of CFP-K2P1 was increased on co-expression of YFP-K2P1 but not with free, cytosolic YFP (Figure 3A, Table S2), consistent with FRET between assembled subunits. Similarly, FRET was observed between K2P1 and K2P3 subunits independent of which subunit carried CFP or YFP, thus demonstrating that these subunits assembled into heteromeric channels (Figure 3B, Table S2). FRET was also observed between co-expressed K2P1 and K2P9 subunits. Confirming expectations based on biochemical studies indicating their assembly (36), FRET was also observed between K2P3 and K2P9 regardless of which subunit carried CFP or YFP. Of note, whole-cell patch-clamp recording demonstrated that like K2P1 (12), K2P3 and K2P9 channels remained fully operational with N- or C-terminal CFP or YFP tags (Figure S4D).

K2P2 did not form heteromeric channels with K2P1, K2P3, or K2P9 regardless of which subunit carried the acceptor or donor fluorescent protein (Figures 3B and S4B, Table S2). Showing that K2P2 subunits can assemble to form homodimeric channels, FRET was observed between CFP-K2P2 and YFP-K2P2 or YFP-K2P23Δ, an alternatively translated, truncated variant found in rat cerebellum (37). The inability of K2P2 and K2P1 to assemble may explain why native K2P2 and SUMO1 did not interact in cerebellar granule neurons (Figure 1).

K2P1 subunits form stable protein-protein complexes with K2P3 or K2P9 subunits

Further evidence for the formation of mixed K2P channels with K2P1 and K2P3 or K2P9 was provided by co-purification of the subunits in detergent stable complexes, as previously reported for K2P3 and K2P9 by others (36). We heterologously expressed K2P3 or K2P9 carrying a nine residue C-terminal tag (1d4) with untagged K2P1 in COS7 cells. Following solubilization, K2P1 was purified when co-expressed with K2P3-1d4 or K2P9-1d4 if immunoprecipitation was carried out with an anti-1d4 antibody, thus confirming mixed subunit assemblies (Figure 3C). Similar to K2P3 or K2P9 bearing C-terminal fluorescent proteins (Figure S4D), the channels tolerated insertion of the 1d4 tag (Figure S4E).

FRET shows that K2P1 is required to recruit SUMO1 into channels with K2P3 or K2P9

Antibody-mediated FRET provided evidence for the close association of native SUMO1 and K2P3 or K2P9 but not K2P2 in cerebellar granule neurons (Figure 1). In CHO cells, K2P3 and K2P9 required K2P1 as an intermediary to interact with SUMO1 (Figure 4A). Heterologously-expressed YFP-SUMO1 failed to interact with CFP-K2P3, CFP-K2P9 and CFP-K2P2; thus, donor decay time constants (τ) were not different from those measured with YFP-SUMO1$_{95}$ (12), a SUMO1 variant unable to link to targets (Figure 4, Figure S4C and Table S3). However, when we coexpressed wild-type K2P1 without a fluorescent protein tag, YFP-SUMO1 interacted with CFP-K2P3 or CFP-K2P9 producing FRET signals as strong as those between homologous channel subunits (YFP-K2P3 and CFP-K2P3 or YFP-K2P9 and CFP-K2P9) (Figure 4B). K2P1-K274Q, a subunit lacking the required Lys residue (12), did not mediate FRET between YFP-SUMO1 and CFP-K2P3 or CFP-K2P9 (Figure 4B), thus showing that recruitment of YFP-SUMO1 into the complexes required a K2P1 subunit subject to sumoylation.

NIH-PA Author Manuscript

NIH-PA Author Manuscript

NIH-PA Author Manuscript

One SUMO is required to silence mixed subunit channels formed with K2P1

K2P1 heterologously-expressed in CHO cells with K2P3 or K2P9 and studied in whole-cell mode produced SENP1-dependent currents consistent with heteromeric channel assembly (Figure S5). Thus, mean current density for K2P1 with K2P3 at +50 mV was 260 ± 36 pA/pF, which was increased by ~200% (550 ± 90 pA/pF) with SENP1 in the pipette. The mean current density of K2P1 with K2P9 increased to a similar extent in response to SENP1. To validate the conclusion of subunit-mixing studies (that are subject to confounding variables such as different rates of subunit turn-over or biased assembly of transfected K2P subunits), we evaluated channels with engineered subunit compositions. Previously, we used this strategy to show that channels formed by two wild-type K2P1 subunits linked in tandem (WT-WT) operated normally and thus were silenced by one SUMO1 monomer although subject to modification on both Lys^{274} residues in the channel complex whereas heterodimeric channels formed by wild-type K2P1 and K2P1-K274Q (WT-Q or Q-WT) functioned similarly but carried at most one SUMO1 monomer (12).

We first expressed K2P1 and K2P3 as a single concatenated protein to create WT–K2P3 channels (Figure 5A). These channels were silent until SENP1 was applied. In excised membrane patches, pretreatment currents were 15 ± 5 pA at +50 mV and SENP1 application increased currents to 410 ± 18 pA. Similar to K2P1 channels, WT–K2P3 channels were silenced on application of SUMO1. Re-application of SENP1 again restored currents. Reversing the order of concatenation to produce K2P3–WT channels did not alter the findings (Figure S6). Similarly, WT–K2P9 and K2P9–WT channels were silent at baseline, were activated by SENP1, were re-silenced by SUMO1, and were re-activated by SENP1 (Figure 5B). Like K2P1 channels without Lys^{274} sites (12), concatenated channels formed by Q-K2P3 or Q-K2P9 subunits were constitutively active and were insensitive to both SUMO1 and SENP1 (Figure 5, A and B). SUMO2 had the same impact as SUMO1 on WT-K2P3 (Figure S6).

To determine the number of SUMO1 molecules linked to single channels, we employed total internal reflection fluorescence (TIRF) microscopy to visualize particles with GFP-SUMO1 at the plasma membrane of living CHO cells and to count associated GFP-SUMO1 monomers by photobleaching (12, 34). As previously reported, K2P1 channels expressed with GFP-SUMO1 showed two bleaching steps for 85% of single particles and one step in 15% of cases (Figure 5C). Because 10–15% of bleaching steps are missed when GFP is studied by photobleaching with this time resolution (38), our data showed that almost all homodimeric K2P1 channels carried two SUMO monomers.

In contrast to K2P1 channels, photobleaching of GFP-SUMO1 expressed with channels formed by linked subunits to produce WT–K2P3 or WT–K2P9 channels showed only one bleaching step per particle in every case (Figure 5C). These data indicated that no more than one SUMO1 monomer was present on a heteromeric, K2P1-containing channel. No fluorescent particles were observed at the CHO cell surface when GFP-SUMO1 was expressed with Q–K2P3 or Q–K2P9 channels. These latter findings demonstrated that Lys^{274} in K2P1 was required for stable interaction of SUMO1 with the channels and that no other sites on WT–K2P3 or WT–K2P9 subunits were sumoylated. Counting one SUMO1 on channels formed by WT–K2P3, WT–K2P9, K2P3–WT or K2P9–WT, also ruled out the possibility that the channels being studied were formed from two K2P1 subunits that had assembled from two separate concatemeric proteins.

A K2P1 pore mutant that acts by blocking current through mixed subunit channels

As an additional tool to evaluate the impact of individual subunits in heteromeric channels, a single change was made in the second P loop of K2P1 (Y231F) which, based on work by

NIH-PA Author Manuscript

NIH-PA Author Manuscript

NIH-PA Author Manuscript

others studying K2P3 (36), was expected to block conduction through channels formed with wild-type subunits. As anticipated, K2P1-Y231F subunits expressed with wild-type K2P1 suppressed SENP1-activated currents at +50 mV by over 90% (Figure 6A). This mutant further demonstrated that K2P1 coassembled with K2P3 or K2P9 but not K2P2: K2P1-Y231F diminished K2P3 and K2P9 currents as strongly as it did K2P1 but did not alter the magnitude of K2P2 currents. FRET studies revealed that CFP-K2P1-Y231F subunits formed stable complexes at the surface of CHO cells with YFP-K2P1, YFP-K2P3 and YFP-K2P9 but not YFP-K2P2 (Figure S7), thus demonstrating that the mutation did not alter subunit trafficking or channel assembly.

Channels with K2P1 and K2P9 are the most responsive to halothane

Because the volatile anesthetic halothane augments currents mediated by K2P3 and K2P9 in homomeric and heteromeric channels, thereby decreasing excitability (28), we sought to determine the influence of halothane on K2P1-containing channels in CHO cells. Halothane augmented K2P3 and K2P9 channel currents by 17% and 30%, respectively (Figure 6B). K2P1 channels silenced by sumoylation were not activated by halothane. SENP1-activated channels formed by K2P1 or WT–K2P3 subunits were augmented by halothane by 5% and 10%, respectively (Figure 6B). In contrast, halothane augmented SENP1-activated, WT–K2P9 channel currents by ~320%. The halothane response series was therefore WT–K2P9 $\gg$ K2P9 > K2P3 > WT–K2P3 or K2P1. These findings suggested that all K2P1-containing channels in neurons were unable to respond to halothane unless they were first desumoylated.

Channels that pass the acid-sensitive portion of IKso can incorporate K2P1

To estimate the contribution of K2P1 subunits to neuronal IKso we applied the methods used to study the channels in CHO cells. First, we confirmed that heterologously expressed fluorescent protein-tagged subunits interacted in neurons as detected by FRET analysis. As in CHO cells, over-expressed YFP-SUMO1 failed to produce a significant FRET signal with CFP-K2P3 or CFP-K2P9 in live cerebellar granule neurons unless wild-type K2P1 was co-expressed; moreover, neither YFP-SUMO1$_{95}$ nor K2P1-K274Q, the variants unable to mediate covalent linkage of SUMO1 and K2P1, produced significant FRET signals (Figure 7A, Table S3).

Next, we used electrophysiology to assess the contribution of endogenous K2P1 to IKso in cerebellar granule neurons. Consistent with SUMO-dependent silencing of K2P1-containing channels at baseline, SUMO1 in the pipette did not alter the magnitude of IKso, Vm or R_{IN} (Figures 2A and 7B). In contrast, SENP1 increased IKso, hyperpolarized Vm and decreased R_{IN}, which reflected that ~50% of IKso was held silent at the surface by the SUMO pathway. In contrast, heterologous-expression of K2P1-Y231F suppressed ~80% of the current measured with SENP1, the same suppression seen with acidification to pH 6.4 (Figures 2A and 7B). This indicates that native subunits capable of interacting with K2P1-Y231F (including K2P1, K2P3 and K2P9 but not K2P2) are fully responsible for the portion of IKso that is acid-sensitive. Because K2P1-Y231F suppressed IKso, Vm, and R_{IN} to the same extent in the presence or absence of SENP1, ~50% of baseline IKso is most likely carried by channels with K2P3 or K2P9 and without K2P1 (Figures 7B and S7B). It seems possible that partner subunits for K2P1 in cerebellar granule neurons are limited to K2P3 and K2P9 given that they share with K2P1 both pore-lining sequences that mediate acid-sensitivity (which are not present in the other K2P channels) and analogous tissue distribution. Further, K2P3 and K2P9 are the only K2P subunits that have been previously demonstrated to form heteromeric channels (15). FRET analysis indicated that CFP-K2P1-Y231F interacted with YFP-tagged SUMO1, K2P1, K2P3 and K2P9 (but not K2P2 or

NIH-PA Author Manuscript

NIH-PA Author Manuscript

NIH-PA Author Manuscript

$SUMO1_{95}$) at the surface of CHO cells (Figure S7A) suggesting that CFP-K2P1-Y231F could also suppress IKso when over-expressed in cerebellar granule neurons.

Channels that respond to halothane can incorporate K2P1

In the absence of added SENP1 to keep K2P1-containing channels silent, halothane increased IKso from 250 to 500 pA/pF (Figure 7C). With SENP1, halothane increased IKso from 500 pA/pF to ~1000 pA/pF. We attributed the 2-fold increase in the absolute magnitude of the halothane effect mostly to heteromeric channels with K2P1 and K2P9 given the low sensitivity of K2P1 and WT-K2P3 channels. That augmentation of IKso by halothane was abolished by heterologous-expression of K2P1-Y231F subunits indicated that the response to the anesthetic was mediated entirely by channels able to incorporate K2P1 (Figures 7C and S6B).

DISCUSSION

Over the past decade, TASK channels with K2P3 or K2P9 subunits have been linked to the physiology of multiple tissues in the nervous system, including in cerebellar granule neurons (26), motorneurons (19), the carotid body (20), the brainstem (39) and the tongue (40). A role for TASK channels has also been shown in the cardiovascular system (21, 41–43), in control of normal cellular lifespan (44) and oncogenesis (45). Although K2P1 is also detected in these tissues it had not been attributed an explicit role in function or pathophysiology until recently (46, 47). Here, we showed that K2P1 formed channels with K2P3 or K2P9 and that the SUMO pathway suppressed the activity of the mixed complexes. We anticipate that the many locations in the body where K2P1 is found with K2P3 or K2P9 will demonstrate this same regulatory mechanism.

Using single transcript analysis we showed the simultaneous presence of the mRNAs for *KCNK1*, *KCNK3* and *KCNK9* in individual rat cerebellar granule neurons. We developed a technique to visualize transcripts of a given type in individual neurons because *in situ* hybridization of rat brain slices had shown overlapping tissue distribution of *KCNK* genes in multiple regions of the brain, including the cerebellum, the amygdala, the neocortex, the piriform cortex and the olfactory bulb (18), but left uncertain which *KCNK* genes were expressed in the same cells. Although transcript data are not yet available for other cell types or species, *KCNK1*, *KCNK3* and *KCNK9* transcripts show the same pattern of tissue expression in many human tissues including the cerebellum, cerebral cortex, prostate, spinal cord (48), cardiac atrium and purkinje fibers (49) suggesting that our observations in rat will apply to humans.

Neurons in the cerebellum are proposed to play a central role in the clinical response to general anesthesia because they control sensorimotor coordination and muscular tone. Thus, halothane augments IKso, thereby decreasing neuronal excitability. We showed that in rat cerebellar granule neurons channels with K2P1, K2P3 and K2P9 produced 80% of IKso and that the response to halothane was mediated entirely by these K2P channels; the residual 20% of IKso was unresponsive to the volatile anesthetic. The effect of halothane on cloned K2P channels and native IKso was reversible and proceeded with roughly the same kinetics as proton blockade; this is consistent with the idea that the action of halothane on ion channels is direct (50). Incorporation of K2P1 into IKso channels led to suppression of ~50% of the current in resting neurons and halothane did not activate SUMO-silenced native or cloned, homomeric or heteromeric channels.

We showed that channels formed by K2P1 and K2P3 or K2P9 remained silent even in off-cell membrane patches until they were desumoylated and that regulation was through linkage of one SUMO moiety. The results obtained with CHO cells and rat cerebellar

NIH-PA Author Manuscript

NIH-PA Author Manuscript

NIH-PA Author Manuscript

granule neurons are consistent with our prior work with Xenopus oocytes, CHO cells and hippocampal neurons where SUMO1, SUMO2, SUMO activating enzyme (SAE1) and SUMO conjugase (ubc9) are found at the plasma membrane and activity of the pathway can be studied in excised membrane patches (12, 33, 34).

K2P1 is not present in cultured hippocampal neurons, and SUMO regulates the excitability of these cells through the voltage-gated potassium channel Kv2.1 (34). Although one SUMO moiety on a K2P1-containing channel has an all-or-none impact, Kv2.1 channels show a stepwise shift in the voltage required to activate so that the rate of action potential firing is increased in a graded fashion by modification of one or two sites (34). Similar to K2P1 in rat cerebellar granule neurons, antibody-mediated FRET studies show that Kv2.1 channels at the hippocampal cell surface are sumoylated (34). In addition, sumoylation has been shown to decrease kainate-receptor mediated excitatory postsynaptic currents in hippocampal neurons by increasing endocytosis of GluR6 subunits (51).

Although correlation of native TASK-like currents and clones has been challenging (15), our results suggest that the diversity of TASK-like conductances recorded in neurons (52) can be understood at least in-part by coassembly of K2P1 with K2P3 or K2P9. It is also helpful that K2P1 can now be identified as a potassium-selective leak channel sensitive to pH (through the same mechanism as for K2P3 and K2P9) and held silent by sumoylation (12, 33), rather than a pH insensitive, weak inward rectifier (TWIK) (53). It is important to note that K2P1 operates as a TASK-like subunit, assembling with K2P3 or K2P9 and exhibiting proton block through the same pore motif, but shares close sequence homology with the bona fide TASK subunits only in the first P domain.

It remains uncertain how cells control SUMO pathway activity. Proteomic studies have required strong stimuli such as heat shock, osmotic challenge and oxidative stress to demonstrate changes in cultured cells and induce global perturbations in sumoylation of targets (54, 55). K2P1-bearing channels are constitutively sumoylated at the surface of CHO cells, Xenopus oocytes and rat cerebellar granule neurons whereas Kv2.1 channels show partial modification in CHO cells and hippocampal neurons (12, 33, 34). We postulate that cells have mechanisms to tune activity of the SUMO pathway for example to allow cerebellar granule neurons to regulate their responses to neurotransmitters, pungent agents, volatile anesthetics and changes in pH and pO_2.

MATERIALS and METHODS

Molecular biology

Human K2P1 (NP_002236), K2P2 (NP_001017424), K2P3 (NP_002237) and K2P9 (NP_057685) were subcloned into pMAX, a laboratory vector with a CMV promoter for mammalian expression. The homology of the human and rat variants is 96% for K2P1, 91% for K2P3 and 85% for K2P9, so we do not anticipate substantial differences between the variants. Human clones were used for electrophysiology, FRET and co-immunopurification experiments. Rat clones were employed to validate the specificity of primary antibodies used in antibody-mediated FRET studies. Tandem constructs were made by introducing the BsrG1I restriction site after the start codon and before the stop codon of each subunit. Following digestion with BsrG1, appropriate fragments were religated and sequenced. Mutations were introduced with *Pfu* Quikchange PCR (Stratagene, CA) and YFP, CFP and 1d4 epitope tagged variant genes were generated as before (12). Lipofectamine 2000 (Invitrogen) was used to transfect cells with plasmids for study 24 to 48 hr later.

NIH-PA Author Manuscript

NIH-PA Author Manuscript

NIH-PA Author Manuscript

Cell Culture and heterologous expression

CHO and COS7 cells (ATCC, VA) were maintained in F12 and DMEM medium, respectively, supplemented with 10% FBS (Invitrogen, CA). Rat cerebellar granule neurons were cultured from 6 to 8 day old pups as previously described (27). Briefly, the cerebellum was isolated, cut into 300 μm cubes, triturated with a fire-polished Pasteur pipette and incubated for 15 min at 37°C with 2.5 mg/ml trypsin in phosphate buffered saline (PBS). Digestion was halted by the addition of PBS containing 0.1 mg/ml soybean trypsin inhibitor, 2000 U/ml DNase I and 1 mM $MgCl_2$. Cells were pelleted by centrifugation for one min at 100 g and resuspended in MEM supplemented with 10% FBS, 26 mM glucose, 19 mM KCl and 2 mM L-glutamine. The cells were seeded on poly-L-lysine–coated 15 mm coverslips and incubated in a humidified atmosphere containing 5 % CO_2 / 95 % air at 37°C. After 48 hours, the culture medium was exchanged for one consisting of MEM supplemented with 10% horse serum, 26 mM glucose, 19 mM KCl, 2 mM L-glutamine and 80 μM L-fluorodeoxyuridine to prevent proliferation of non-neuronal cells. Culture medium was exchanged every 3 days. Cells were studied between days 7 and 10 in culture at room temperature.

Biochemistry

COS7 cells were grown in 15 cm plates, transfected and then harvested 24 hrs later in IP buffer containing 1% Triton X-100, 0.1% SDS, 1mM EDTA, 100mM NaCl and Tris-HCl at pH 7.5. Lysates were homogenized on ice for 30 min, incubated at 4°C for one hour and then centrifuged at 13,000 g for 20 min. Supernatants were incubated overnight at 4°C with 5 μg/ml mouse anti-Id4 antibody (University of British Columbia) before the addition of Protein-G Sepharose (GE Healthcare, NJ). Material was run over a Nickel NTA Agarose column (Qiagen, CA) and washed with IP buffer containing 900 mM NaCl. K2P subunits were eluted with sample buffer containing: 50 mM Tris-HCl pH 6.8, 2% SDS, 10% glycerol, 0.02 % bromophenol blue, 12.5 mM EDTA, 50 mM DTT. Samples were incubated at 70°C for 4 min, separated on a 4–20 % polyacrylamide gel and transferred to a nitrocellulose membrane. K2P1 monomers were detected at ~38 kDa with rabbit anti-K2P1 antibody (1: 2000, Santa Cruz, CA) and 1d4-tagged K2P3 and K2P9 monomers were detected at ~44 kDa and ~42 kDa, respectively, with mouse anti-Id4 antibody (1:2000) using secondary antibodies raised in goat and conjugated to horse-radish peroxidase (1:300,000 BioRad, CA), followed by ECL Advance chemiluminesence (GE Healthcare, NJ).

FRET Immunocytochemistry

Double immunostaining for SUMO1 and K2P1, or K2P3, or K2P9, or K2P2 was performed to assess FRET using secondary antibodies labeled with Alexa 594 to visualize SUMO1 and Alexa 488 to label the K2P subunit, as used previously for Kv2.1 voltage-gated potassium channel subunits (34). Cells were permeabilized with digitonin (20 mg/ml) in a HEPES-buffered solution containing a cocktail of protease inhibitors (*N*-methylmaleimide, PMSF, aprotinin, leupeptin, antipain, and pepstatin A), and then fixed in 2% paraformaldehyde for 30 min. Cells were incubated with a rabbit polyclonal antibody raised against amino acids 86–97 of human SUMO1 (3 μg/ml, Sigma-Aldrich). SUMO1 binding was detected with highly cross-adsorbed donkey anti-rabbit IgG (1 μg/ml, Invitrogen) labeled with Alexa 594 to act as the FRET acceptor. K2P subunits were identified with subunit-specific polyclonal goat antibodies (4 μg/ml, Santa Cruz Biotechnology, Santa Cruz, CA). The antibodies were raised to a peptide mapping near the C-terminus of human K2P1; a peptide mapping near the C-terminus of human K2P3; a peptide mapping near the C-terminus of rat K2P9; a peptide mapping near the C-terminus of human K2P2. Anti-K2P antibody binding was detected with highly cross-adsorbed donkey anti-goat IgG (1 μg/ml, Invitrogen) labeled with Alexa 488 to serve as the FRET donors. Cell nuclei were labeled with DAPI. To confirm there was no

NIH-PA Author Manuscript

NIH-PA Author Manuscript

NIH-PA Author Manuscript

confounding cross-reactivity between K2P subunit antibodies, labeling studies were performed in CHO cells over-expressing K2P1, K2P3, or K2P9 (Figure S2).

Cells were imaged with a 60x, NA 1.40 oil objective on a Leica SP5 laser scanning confocal microscope with identical illumination acquisition settings across staining conditions. Sequential images of Alexa 488 and Alexa 594 were obtained using laser lines at 488 nm and 546 nm. DAPI illumination was achieved with two-photon illumination at 750 nm. The Leica Acceptor Photobleaching Wizard was used to obtain pre-bleach images of K2P subunit intensities (Alexa 488) and SUMO1 (Alexa 594); to define a region on the K2P subunit image; to bleach the Alexa 594 fluorescence within the region by 200 passes at full laser power; and, to obtain post-bleaching images of Alexa 488 and Alexa 594 fluorescence. Image pairs demonstrating any shift in focus between pre- and post-bleaching images were excluded. Twelve bit raw confocal images were processed using Huygens Deconvolution software (Scientific Volume Image, Netherlands) and maximum likelihood estimation with a signal to-noise ratio of 20. Raw Alexa 488 images were de-noised using ImageJ (NIH), and FRET efficiency images within the bleaching regions were created on a pixel-by-pixel basis by subtraction of pre-bleach from post-bleach intensity and then division of the difference by the post-bleach intensity. FRET efficiency by this method depends on distance and the degree of saturation of antigen with antibody; therefore, FRET intensities cannot be used to determine the distance between acceptor and donor or to directly compare K2P1, K2P3 and K2P9 images because each subunit is recognized by a different antibody.

Visualization of the mRNA encoding K2P in single neurons

Probe sets to detect rat *KCNK1*, *KCNK3* and *KCNK9* mRNAs, amplifying reagents and fluorescent tags were purchased (ViewRNA Assay, Affymetrix, CA). The probe sets are designed to target two adjacent and unique sequences in each mRNA message and specific signals are produced because amplicons are visualized only when both adjacent probes bind to the mRNA. *KCNK1*, *KCNK3* and *KCNK9* were labeled with Cy3, Cy5 and Cy7, respectively. Fixation, hybridization, amplification and fluorescent labeling were performed according per the instructions and as reported (56, 57) using cerebellar granule neurons on day 10 in culture. Cells were visualized using a Leica SP5 laser scanning confocal microscope with a 100x, 1.40 NA objective and laser scanning set to produce 30 nm^2 per pixel. Cells were sequentially illuminated on a line-by-line basis to excite each fluorophore. Thin confocal sections extending from the cover glass to the top pole of the cells were obtained. Twelve bit raw confocal images were processed in the same manner as for FRET Immunochemistry (above). Reconstructions in 3D were produced using ImageJ. Puncta representing *KCNK1*, *KCNK3* and *KCNK9* mRNA transcripts were identified as 3D particles and measured using the 3D Particle Counter plug-in in Fiji, an open source processing package based on ImageJ.

Electrophysiology

An Axopatch 200B amplifier and pCLAMP software (Molecular Devices, CA) at filter and sampling frequencies of 5 and 25 kHz were used. For whole-cell recording, cells were superfused with solution A (in mM): NaCl 140, KCl 4, $CaCl_2$ 1.0, $MgCl_2$ 1.0, glucose 5.5, HEPES 10. The pH was adjusted as appropriate with NaOH and HCl. Cells were studied at room temperature with borosilicate glass pipettes (Clark, UK) with a resistance of 4 – 5 MΩ when filled with solution B (in mM): KCl 136, $MgCl_2$ 1, K_2ATP 2, EGTA 5, HEPES 10, pH 7.2 with KOH. For excised patch studies, the inside of patches was exposed to solution B and 1.5 – 2 MΩ pipettes were filled with solution A. To study the effects of the SUMO pathway on channel function, 100 pM SUMO1 or 250 pM SENP1 were included in solution B. All recording pipettes were coated with Sigmacote (Sigma, MI). IKso was studied with a modification of a previously published protocol (27): Cells were held at −20 mV for 20 s.

NIH-PA Author Manuscript

NIH-PA Author Manuscript

NIH-PA Author Manuscript

Then, the holding voltage was ramped to −120 mV over a period of 100 ms before returning to −20 mV. Resting membrane potential (Vm), defined as the zero current potential, was determined from current ramps. Cellular input resistance was calculated from the slope of current ramps (approximated to a straight line) evoked between 10 mV positive to and 10 mV negative to the resting membrane potential. Halothane (Sigma, MI) was added to solution A overnight prior to use to a final concentration of 5 mM. Following equilibration, anesthetic solutions were covered tightly with parafilm and superfused at ~2 ml/min.

Live CHO cell FRET

Donor-decay time-course was studied as before (12), using an automated Olympus IX81 epi-fluorescence microscope. CFP was excited at 458 nm and the emission collected through a 470–500 nm bandpass filter, YFP was excited at 514 nm and the emission collected through a 525–575 nm filter. Images were captured using a CCD camera controlled by Metamorph (Molecular Devices) and were analyzed with ImageJ.

Single particle photobleaching

GFP was excited by a 488 nm, 10 mW Argon laser (Melles Griot) and the critical angle for TIRF obtained with a micrometer and a 150x, 1.45NA apochromat objective on an Olympus IX70 microscope. To observe single particles, GFP-fused subunits were expressed at low levels. Constant excitation induced photobleaching and movies of 300–500 frames were acquired at 10 Hz using a back-illuminated EM-CCD camera. Data were analyzed as previously described (34). Average background fluorescence was determined from the first five images, subtracted from the movie, fluorescence summed for a 4 × 4 pixel region around the peak of each particle and analyzed over time with ImageJ and Origin v6 software.

Statistical analysis

Statistical analyses were performed with Prism (GraphPad) using one-way ANOVA. In each dataset demonstrating significant ($p<0.05$) F values, differences within pairs of group means were tested using the Bonferroni posthoc test.

Supplementary Material

Refer to Web version on PubMed Central for supplementary material.

Acknowledgments

We thank V. Bindokas, I.S. Dementieva, E.J. Dowdell and J. Wang for technical support and R. Goldstein and K.J. Ruscic for thoughtful discussions.

Funding: The authors are grateful to the N.I.H. for support R01NS058505 (SANG) and R01 NS056313 (JDM).

REFERENCES AND NOTES

1. Goldman DE. Potential, impedance, and rectification in membranes. J Gen Physiol. 1943; 27:37. [PubMed: 19873371]
2. Hodgkin AL, Katz B. The effect of sodium ions on the electrical activity of the giant axon of the squid. J Physiol. 1949; 108:37. [PubMed: 18128147]
3. Goldstein SAN, Bockenhauer D, O'Kelly I, Zilberberg N. Potassium leak channels and the KCNK family of two-P-domain subunits. Nat Rev Neurosci. 2001; 2:175. [PubMed: 11256078]
4. Plant, LD.; Bayliss, DA.; Kim, D.; Lesage, F.; Goldstein, SAN. IUPHAR database. 2009.

NIH-PA Author Manuscript

NIH-PA Author Manuscript

NIH-PA Author Manuscript

5. Ketchum KA, Joiner WJ, Sellers AJ, Kaczmarek LK, Goldstein SAN. A new family of outwardly-rectifying potassium channel proteins with two pore domains in tandem. Nature. 1995; 376:690. [PubMed: 7651518]
6. Goldstein SAN, Price LA, Rosenthal DN, Pausch MH. ORK1, a potassium-selective leak channel with two pore domains cloned from Drosophila melanogaster by expression in Saccharomyces cerevisiae. Proc Natl Acad Sci. 1996; 93:13256. [PubMed: 8917578]
7. Ilan N, Goldstein SAN. KCNK0: single, cloned potassium leak channels are multi-ion pores. Biophys J. 2001; 80:241. [PubMed: 11159398]
8. Duprat F, Lesage F, Fink M, Reyes R, Heurteaux C, Lazdunski M. TASK, a human background K+ channel to sense external pH variations near physiological pH. EMBO J. 1997; 16:5464. [PubMed: 9312005]
9. Kim D, Fujita A, Horio Y, Kurachi Y. Cloning and functional expression of a novel cardiac two-pore background K+ channel (cTBAK-1). Circ Res. 1998; 82:513. [PubMed: 9506712]
10. Lopes CMB, Zilberberg N, Goldstein SAN. Block of Kcnk3 by Protons: evidence that 2-P-domain potassium channel subunits function as homodimers. J Biol Chem. 2001; 276:24449. [PubMed: 11358956]
11. Kollewe A, Lau AY, Sullivan A, Roux B, Goldstein SAN. A structural model for K2P potassium channels based on 23 pairs of interacting sites and continuum electrostatics. J Gen Physiol. 2009; 134:53.10.1085/jgp.200910235 [PubMed: 19564427]
12. Plant LD, Dementieva IS, Kollewe A, Olikara S, Marks JD, Goldstein SA. One SUMO is sufficient to silence the dimeric potassium channel K2P1. Proc Natl Acad Sci. 2010; 107:10743. [PubMed: 20498050]
13. Miller AN, Long SB. Crystal structure of the human two-pore domain potassium channel K2P1. Science. 2012; 335:432. published online EpubJan 27. 10.1126/science.1213274 [PubMed: 22282804]
14. Brohawn SG, del Marmol J, MacKinnon R. Crystal structure of the human K2P TRAAK, a lipid- and mechano-sensitive K+ ion channel. Science. 2012; 335:436. published online EpubJan 27. 10.1126/science.1213808 [PubMed: 22282805]
15. Enyedi P, Czirják G. Molecular Background of Leak K+ Currents: Two-Pore Domain Potassium Channels. Physiol Rev. 2010; 90:559.10.1152/physrev.00029.2009 [PubMed: 20393194]
16. Lopes CMB, Gallagher PG, Buck ME, Butler MH, Goldstein SAN. Proton block and voltage-gating are potassium-dependent in the cardiac leak channel Kcnk3. J Biol Chem. 2000; 275:16969. [PubMed: 10748056]
17. Rajan S, Wischmeyer E, Liu GX, Muller RP, Daut J, Karschin A, Derst C. TASK-3, a novel tandem pore domain acid-sensitive K+ channel - An extracellular histidine as pH sensor. J Biol Chem. 2000; 275:16650. [PubMed: 10747866]
18. Talley EM, Solorzano G, Lei Q, Kim D, Bayliss DA. CNS distribution of members of the two-pore-domain (KCNK) potassium channel family. J Neurosci. 2001; 21:7491. [PubMed: 11567039]
19. Talley EM, Lei QB, Sirois JE, Bayliss DA. TASK-1, a two-pore domain K+ channel, is modulated by multiple neurotransmitters in motoneurons. Neuron. 2000; 25:399. [PubMed: 10719894]
20. Buckler KJ, Williams BA, Honore E. An oxygen-, acid- and anaesthetic-sensitive TASK-like background potassium channel in rat arterial chemoreceptor cells. J Physiol (Lond). 2000; 525:135. [PubMed: 10811732]
21. Leonoudakis D, Gray AT, Winegar BD, Kindler CH, Harada M, Taylor DM, Chavez RA, Forsayeth JR, Yost CS. An open rectifier potassium channel with two pore domains in tandem cloned from rat cerebellum. J Neurosci. 1998; 18:868. [PubMed: 9437008]
22. Gurney AM, Osipenko ON, MacMillan D, McFarlane KM, Tate RJ, Kempsill FEJ. Two-Pore Domain K Channel, TASK-1, in Pulmonary Artery Smooth Muscle Cells. Circ Res. 2003; 93:957. published online EpubNovember 14, 2003. 10.1161/01.res.0000099883.68414.61 [PubMed: 14551239]
23. Czirjak G, Fischer T, Spat A, Lesage F, Enyedi P. TASK (TWIK-related acid-sensitive K+ channel) is expressed in glomerulosa cells of rat adrenal cortex and inhibited by angiotensin II. Molecular Endocrinology. 2000; 14:863. [PubMed: 10847588]

NIH-PA Author Manuscript

NIH-PA Author Manuscript

NIH-PA Author Manuscript

24. Davies LA, Hu C, Guagliardo NA, Sen N, Chen X, Talley EM, Carey RM, Bayliss DA, Barrett PQ. TASK channel deletion in mice causes primary hyperaldosteronism. Proc Natl Acad Sci. 2008; 105:2203. published online EpubFebruary 12, 2008. 10.1073/pnas.0712000105 [PubMed: 18250325]
25. Meuth SG, Bittner S, Meuth P, Simon OJ, Budde T, Wiendl H. TWIK-related Acid-sensitive K+ Channel 1 (TASK1) and TASK3 Critically Influence T Lymphocyte Effector Functions. J Biol Chem. 2008; 283:14559. published online EpubMay 23, 2008. 10.1074/jbc.M800637200 [PubMed: 18375952]
26. Millar JA, Barratt L, Southan AP, Page KM, Fyffe RE, Robertson B, Mathie A. A functional role for the two-pore domain potassium channel TASK-1 in cerebellar granule neurons. Proc Natl Acad Sci U S A. 2000; 97:3614. [PubMed: 10725353]
27. Plant LD, Kemp PJ, Peers C, Henderson Z, Pearson HA. Hypoxic depolarization of cerebellar granule neurons by specific inhibition of TASK-1. Stroke. 2002; 33:2324. [PubMed: 12215606]
28. Talley EM, Bayliss DA. Modulation of TASK-1 (Kcnk3) and TASK-3 (Kcnk9) Potassium Channels. J Biol Chem. 2002; 277:17733. published online EpubMay 17, 2002. 10.1074/jbc.M200502200 [PubMed: 11886861]
29. Bautista DM, Sigal YM, Milstein AD, Garrison JL, Zorn JA, Tsuruda PR, Nicoll RA, Julius D. Pungent agents from Szechuan peppers excite sensory neurons by inhibiting two-pore potassium channels. Nat Neurosci. 2008; 11:772. [PubMed: 18568022]
30. Kang D, Han J, Talley EM, Bayliss DA, Kim D. Functional expression of TASK-1/TASK-3 heteromers in cerebellar granule cells. J Physiol. 2004; 554:64. published online EpubJanuary 1, 2004. 10.1113/jphysiol.2003.054387 [PubMed: 14678492]
31. Brickley SG, Revilla V, Cull-Candy SG, Wisden W, Farrant M. Adaptive regulation of neuronal excitability by a voltage-independent potassium conductance. Nature. 2001; 409:88. [PubMed: 11343119]
32. Goldstein SAN, Wang KW, Ilan N, Pausch M. Sequence and function of the two P domain potassium channels: implications of an emerging superfamily. J Molec Med. 1998; 76(1):13. [PubMed: 9462864]
33. Rajan S, Plant LD, Rabin ML, Butler MH, Goldstein SAN. Sumoylation silences the plasma membrane leak K^+ channel K2P1. Cell. 2005; 121:37. [PubMed: 15820677]
34. Plant LD, Dowdell EJ, Dementieva IS, Marks JD, Goldstein SAN. SUMO modification of cell surface Kv2.1 potassium channels regulates the activity of rat hippocampal neurons. J Gen Physiol. 2011; 137:441. published online EpubMay 1, 2011. 10.1085/jgp.201110604 [PubMed: 21518833]
35. Watkins CS, Mathie A. A non-inactivating K^+ current sensitive to muscarinic receptor activation in rat cultured cerebellar granule neurons. J Physiol. 1996; 491:401. [PubMed: 8866863]
36. Berg AP, Talley EM, Manger JP, Bayliss DA. Motoneurons express heteromeric TWIK-related acid-sensitive K^+ (TASK) channels containing TASK-1 (KCNK3) and TASK-3 (KCNK9) subunits. J Neurosci. 2004; 24:6693.10.1523/jneurosci.1408-04.2004 [PubMed: 15282272]
37. Thomas D, Plant LD, Wilkens CM, McCrossan ZA, Goldstein SAN. Alternative Translation Initiation in Rat Brain Yields K2P2.1 Potassium Channels Permeable to Sodium. Neuron. 2008; 58:859. [PubMed: 18579077]
38. Ulbrich MH, Isacoff EY. Subunit counting in membrane-bound proteins. Nat Meth. 2007; 4:319.
39. Bayliss DA, Talley EM, Sirois JE, Lei Q. TASK-1 is a highly modulated pH-sensitive 'leak' K^+ channel expressed in brainstem respiratory neurons. Respiration Physiology. 2001; 129:159.10.1016/s0034-5687(01)00288-2 [PubMed: 11738652]
40. Richter TA, Dvoryanchikov GA, Chaudhari N, Roper SD. Acid-sensitive two-pore domain potassium (K2P) channels in mouse taste buds. J Neurophysiol. 2004; 92:1928. [PubMed: 15140906]
41. Kim Y, Bang H, Kim D. TBAK-1 and TASK-1, two-pore K^+ channel subunits: kinetic properties and expression in rat heart. Am J Physiol. 1999; 277:H1669. [PubMed: 10564119]
42. Lopes CM, Gallagher PG, Buck ME, Butler MH, Goldstein SA. Proton block and voltage gating are potassium-dependent in the cardiac leak channel Kcnk3. The Journal of biological chemistry. 2000; 275:16969. published online EpubJun 2. 10.1074/jbc.M001948200 [PubMed: 10748056]

NIH-PA Author Manuscript

NIH-PA Author Manuscript

NIH-PA Author Manuscript

43. Putzke C, Wemhöner K, Sachse FB, Rinné S, Schlichthörl G, Li XT, Jaé L, Eckhardt I, Wischmeyer E, Wulf H, Preisig-Müller R, Daut J, Decher N. The acid-sensitive potassium channel TASK-1 in rat cardiac muscle. Cardiovascular Research. 2007; 75:59. published online EpubJuly 1, 2007. 10.1016/j.cardiores.2007.02.025 [PubMed: 17389142]
44. Lauritzen I, Zanzouri M, Honore E, Duprat F, Ehrengruber MU, Lazdunski M, Patel AJ. K^+-dependent Cerebellar Granule Neuron Apoptosis: Role of TASK Leak K^+ Channels. J Biol Chem. 2003; 278:32068. published online EpubAugust 22, 2003. 10.1074/jbc.M302631200 [PubMed: 12783883]
45. Mu D, Chen L, Zhang X, See LH, Koch CM, Yen C, Tong JJ, Spiegel L, Nguyen KC, Servoss A, Peng Y, Pei L, Marks JR, Lowe S, Hoey T, Jan LY, McCombie WR, Wigler MH, Powers S. Genomic amplification and oncogenic properties of the KCNK9 potassium channel gene. Cancer Cell. 2003; 3:297. [PubMed: 12676587]
46. Ma L, Zhang X, Chen H. TWIK-1 two-pore domain potassium channels change ion selectivity and conduct inward leak sodium currents in hypokalemia. Sci Signal. 2011; 4:ra37. [PubMed: 21653227]
47. Goldstein SAN. K2P Potassium Channels, Mysterious and Paradoxically Exciting. Sci Signal. 2011; 4(184):pe35.10.1126/scisignal.2002225 [PubMed: 21868351]
48. Su AI, Wiltshire T, Batalov S, Lapp H, Ching KA, Block D, Zhang J, Soden R, Hayakawa M, Kreiman G, Cooke MP, Walker JR, Hogenesch JB. A gene atlas of the mouse and human protein-encoding transcriptomes. Proc Natl Acad Sci. 2004; 101:6062. published online EpubApril 20, 2004. 10.1073/pnas.0400782101 [PubMed: 15075390]
49. Gaborit N, Le Bouter S, Szuts V, Varro A, Escande D, Nattel S, Demolombe S. Regional and tissue specific transcript signatures of ion channel genes in the non-diseased human heart. J Physiol. 2007; 582:675. published online EpubJuly 15, 2007. 10.1113/jphysiol.2006.126714 [PubMed: 17478540]
50. Shin WJ, Winegar BD. Modulation of noninactivating K+ channels in rat cerebellar granule neurons by halothane, isoflurane, and sevoflurane. Anesth Analg. 2003; 96:1340. published online Epub2003/04/23. [PubMed: 12707130]
51. Martin S, Nishimune A, Mellor JR, Henley JM. SUMOylation regulates kainate-receptor-mediated synaptic transmission. Nature. 2007; 447:321. [PubMed: 17486098]
52. Han J, Truell J, Gnatenco C, Kim D. Characterization of four types of background potassium channels in rat cerebellar granule neurons. J Physiol. 2002; 542:431. [PubMed: 12122143]
53. Lesage F, Guillemare E, Fink M, Duprat F, Lazdunski M, Romey G, Barhanin J. TWIK-1, a ubiquitous human weakly inward rectifying K+ channel with a novel structure. EMBO J. 1996; 15:1004. [PubMed: 8605869]
54. Bossis G, Melchior F. Regulation of SUMOylation by Reversible Oxidation of SUMO Conjugating Enzymes. Molecular Cell. 2006; 21:349. [PubMed: 16455490]
55. Gareau JR, Lima CD. The SUMO pathway: emerging mechanisms that shape specificity, conjugation and recognition. Nat Rev Mol Cell Biol. 2010; 11:861. [PubMed: 21102611]
56. Ting DT, Lipson D, Paul S, Brannigan BW, Akhavanfard S, Coffman EJ, Contino G, Deshpande V, Iafrate AJ, Letovsky S, Rivera MN, Bardeesy N, Maheswaran S, Haber DA. Aberrant overexpression of satellite repeats in pancreatic and other epithelial cancers. Science. 2011; 331:593. published online EpubFeb 4. 10.1126/science.1200801 [PubMed: 21233348]
57. Louzada S, Adega F, Chaves R. Defining the Sister Rat Mammary Tumor Cell Lines HH-16 cl.2/1 and HH-16.cl.4 as an In Vitro Cell Model for Erbb2. PLoS ONE. 2012; 7:e29923.10.1371/journal.pone.0029923 [PubMed: 22253826]

NIH-PA Author Manuscript
NIH-PA Author Manuscript
NIH-PA Author Manuscript

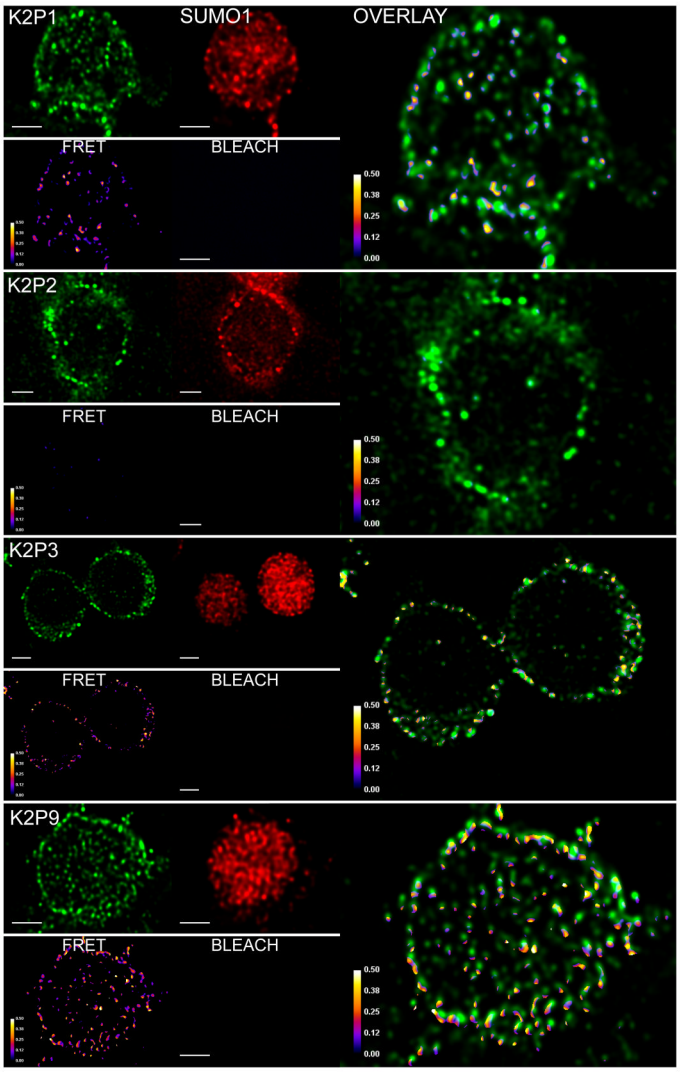

Figure 1. Interaction of native proteins at the neuronal surface: FRET between SUMO1 and K2P1, SUMO1 and K2P3, SUMO1 and K2P9, but not SUMO1 and K2P2

FRET in CGN was performed using antibodies to K2P1, K2P2, K2P3, or K2P9 to tag them with the donor fluorophore (green) and antibodies to label SUMO1 with the acceptor (red). Images are representative of 5–6 fields of view per K2P channel. Each row shows four small images of: channel (top left), SUMO1 (top right), SUMO1 after photobleaching (BLEACH), and increased donor fluorescence after photobleaching (FRET); the large panel in each row is an overlay of the channel and the resulting FRET. Images are pseudo-colored to indicate FRET efficiencies calculated for each pixel (calibration bar).

NIH-PA Author Manuscript

NIH-PA Author Manuscript

NIH-PA Author Manuscript

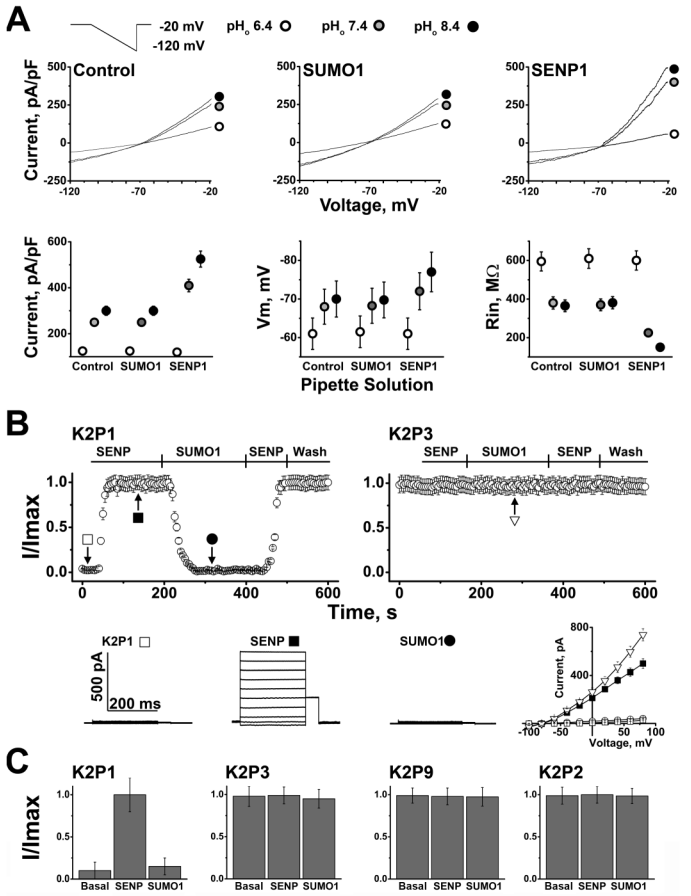

Figure 2. SUMO1 modulates IKso and K2P1 channels but not homodimeric K2P2, K2P3 or K2P9 channels

A. Rat CGN were studied in whole-cell mode with only solution B (control) in the pipette or with SUMO1 or SENP1 added (n = 10 cells). Each cell was perfused with solution A at pH 6.4 (open circle), 7.4 (gray circle) and 8.4 (closed circle). Top, IKso plotted against voltage. Example traces are shown at the top of each row. Bottom, Mean IKso is measured at −20 mV ± SEM (left). Vm is plotted as mean ± SEM (middle). R_{IN} is plotted as mean ± SEM (right). Excitability parameters (IKso, Vm and R_{IN}) are reported in Table S1.

B. Human K2P1 or K2P3 channels heterologously-expressed in CHO cells and studied in inside-out, off-cell patches at 50 mV (normalized mean ± S.E.M, n = 7 patches). Top left, K2P1 channels, negligible basal currents were activated by SENP1 and suppressed by SUMO1. Reapplication of SENP1 restored channel activity despite extended washing (Wash). Top right, K2P3 channels were insensitive to application of SUMO1 and SENP1 (412 ± 36 pA). Bottom, current families and current-voltage relationships at times indicated by symbols.

C. Histograms for normalized current (mean ± SEM) for recordings of K2P1 channels and K2P3 channels in panel B and for K2P9 channels and K2P2 channels when studied as in (B) (n = 7 patches). Unlike K2P1, the other homomeric channels were insensitive to SUMO1 and SENP1 (K2P9 channels, basal 345 ± 32 pA; K2P2 channels, basal 441 ± 43 pA).

NIH-PA Author Manuscript

NIH-PA Author Manuscript

NIH-PA Author Manuscript

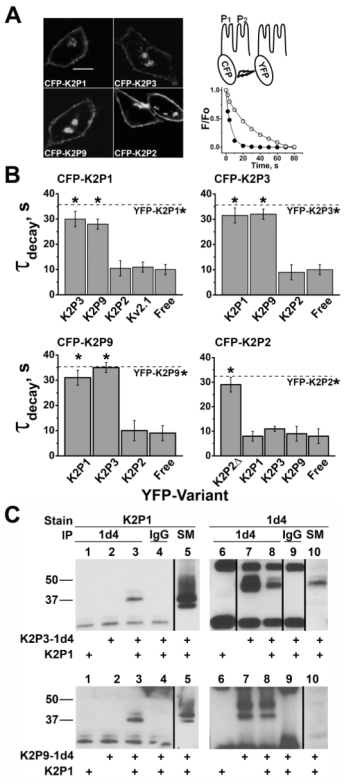

Figure 3. FRET and protein purification both show that K2P1 assembles with K2P3 or K2P9

FRET was studied in live CHO cells. Western blots are representative of 3 experiments.

A. CFP-tagged K2P1, K2P2, K2P3 or K2P9 subunits reach the cell surface (left). Exemplar photobleaching studies (right) show the decay of fluorescence intensity for single cells expressing CFP-K2P1 and YFP-K2P1 (○) or CFP-K2P1 and free YFP (●) fit by an exponential to give τ. Scale bar is 10 μm.

B. FRET shows assembly of CFP-tagged K2P1, K2P3 or K2P9 with YFP-tagged K2P1, K2P3 or K2P9 but not with YFP-K2P2 or free YFP. CFP-K2P1 also did not interact with YFP-Kv2.1. CFP-K2P2 does assemble with YFP-K2P2 and YFP-K2P23Δ. Dotted lines show FRET between CFP and YFP-tagged subunits in homodimeric channels (K2P1, K2P3, K2P9 or K2P2). Significant changes in τ compared to free YFP are indicated (*, $P<0.001$) (Table S2).

C. Assembly of K2P1 and K2P3 (or K2P1 and K2P9) was demonstrated by purification of unlabeled K2P1 (lane 3, ~37 kDa) by 1d4-mediated immunopurification when K2P3-1d4 (top panel) or K2P9-1d4 (bottom panel) was co-expressed; Western blot staining was with antibodies directed to K2P1. Controls: K2P1 was not isolated without K2P3-1d4 or K2P9-1d4 (lane 1); IgG antibodies did not isolate K2P1 (lane 4); staining with anti-1d4 antibodies confirmed K2P3-1d4 or K2P9-1d4 expression (lanes 7 and 8; ~44 and ~42 kDa respectively); starting material (SM) was shown to contain the expressed subunits (lanes 5 and 10). Black lines indicate where interceding lanes have been removed.

NIH-PA Author Manuscript

NIH-PA Author Manuscript

NIH-PA Author Manuscript

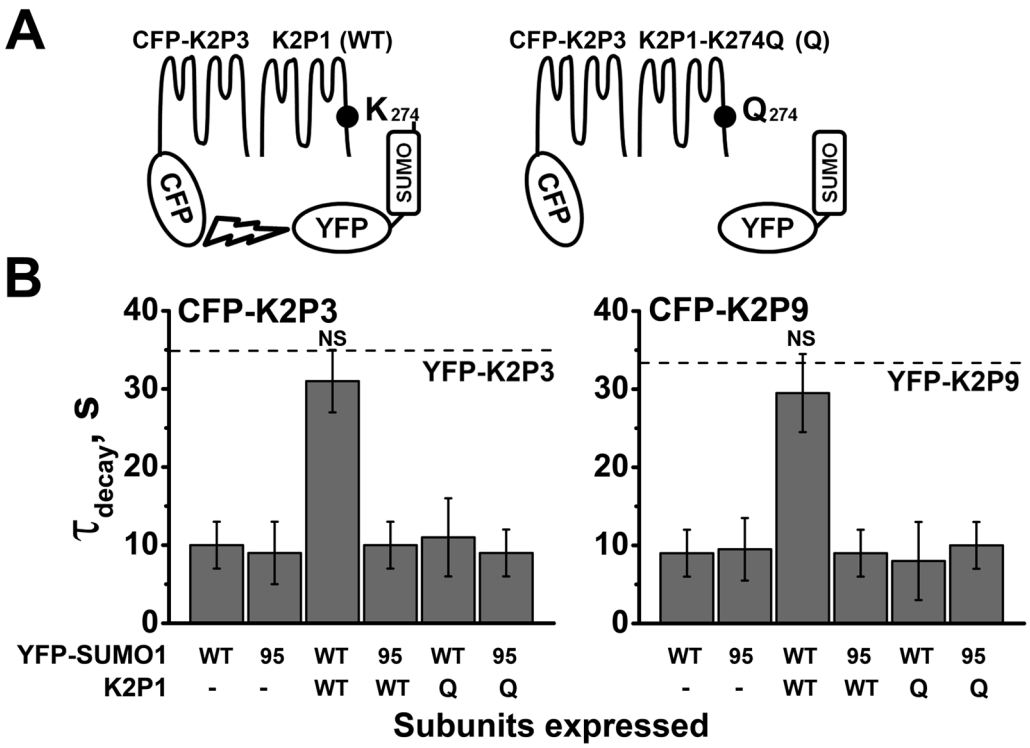

Figure 4. FRET shows that K2P1 recruits SUMO1 into heterodimeric channels with K2P3 or K2P9

Live CHO cells studied as in Figure 3. Fluorescence decay parameters (mean τ ± S.E.M.) are listed in Table S3.

A. Assembly of CFP-K2P3 and wild-type K2P1 (WT) allows FRET with YFP-SUMO1 whereas K2P1-K274Q (Q) precludes both sumoylation and FRET.

B. K2P1 is required for FRET between CFP-K2P3 (or CFP-K2P9) and YFP-SUMO. FRET is observed in homodimeric channels between subunits tagged with CFP and YFP (dotted lines); CFP-K2P3 or CFP-K2P9 show FRET with YFP-SUMO1 only when wild-type K2P1 (WT) is also expressed (NS,, indicates no significant change compared to homodimeric channel FRET signal). Controls: FRET was not observed with a linkage-deficient SUMO, YFP-SUMO1$_{95}$ (95), or a sumoylation-deficient mutant, K2P1-K274Q (Q).

NIH-PA Author Manuscript

NIH-PA Author Manuscript

NIH-PA Author Manuscript

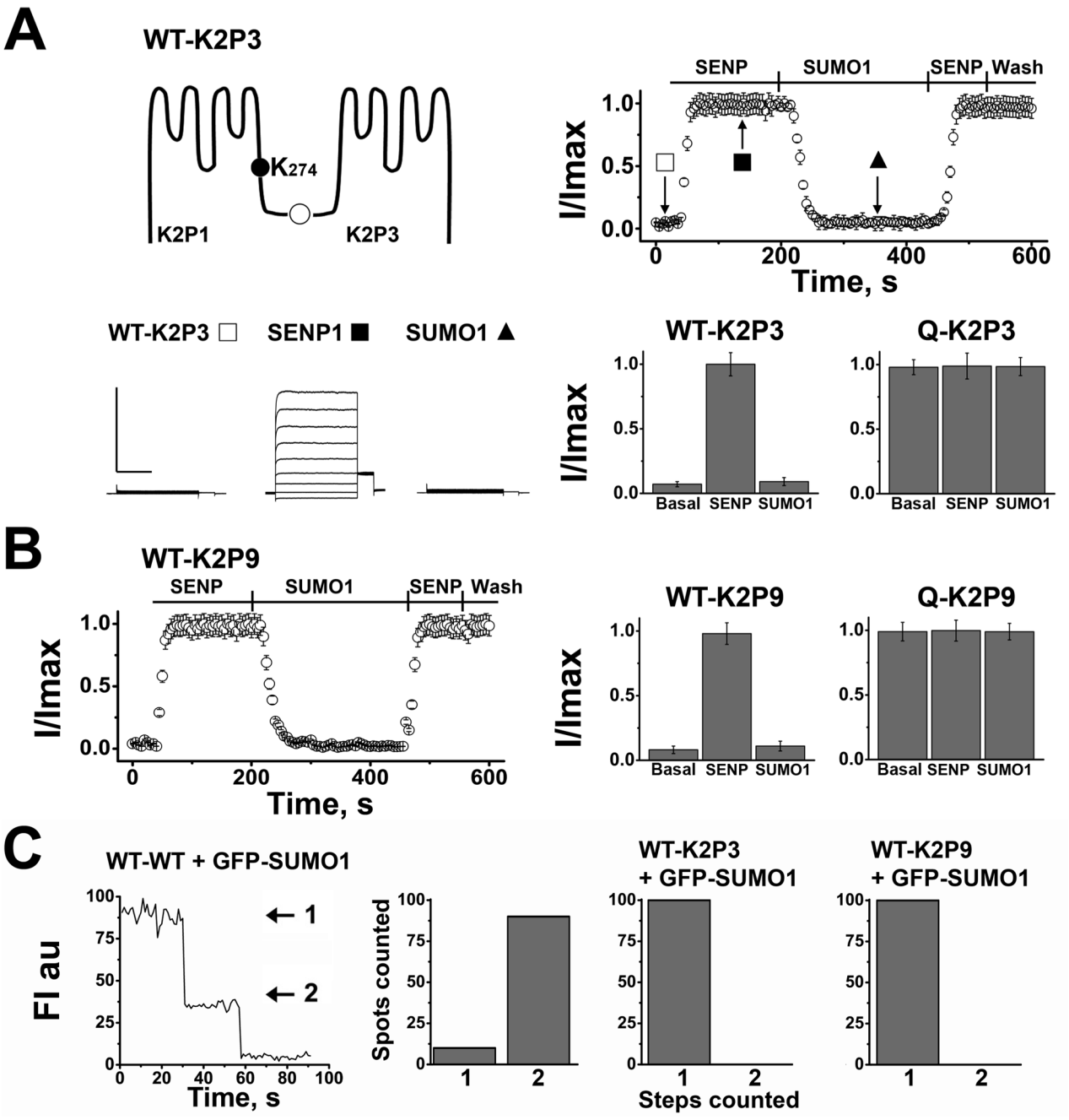

Figure 5. One SUMO moiety is necessary and sufficient to silence heterodimeric tandem channels with K2P1 and K2P3 or K2P9

Channel subunits were heterologously-expressed in CHO cells and studied either as in Figure 2 or using TIRF microscopy to visualize and count GFP-SUMO1 monomers.

A. Top left, WT-K2P3 is a tandem subunit formed by linking wild-type K2P1 (WT) and K2P3 (K2P1-Lys^{274} and the connection point between subunits, open circle, are indicated). Top right, normalized current for WT-K2P3 channels (mean ± S.E.M., n = 5 patches) at 50 mV measured in inside-out, off-cell patches as in Figure 2B. Basal currents (12 ± 4 pA) were activated by SENP1 (305 ± 11 pA) and suppressed by SUMO1. Reapplication of SENP1 restored channel activity despite extended washing (Wash). Bottom left, current

families at times indicated by symbols. Bottom right, histograms showing normalized basal current and after application of SUMO1 and SENP1; Q-K2P3 channels are formed with K2P1-K274Q and K2P3 and do not respond to either SUMO1 or SENP1.

B. Left, WT-K2P9 channels in off-cell patches excised from CHO cells are silent at baseline (10 ± 3 pA) and activated by SENP1 (355 ± 28 pA) when studied as in (A). Right, histograms showing normalized current, basal and on application of SUMO1 and SENP1; Q-K2P9 channels are formed with K2P1-K274Q and K2P9 and do not respond to SUMO1 or SENP1.

C. GFP-tagged SUMO1 was studied at the CHO cell surface by TIRF. Left, a representative single, fluorescent GFP-K2P1 particle showing two photobleaching steps. Right, histogram showing that 90% of 90 GFP-K2P1 particles demonstrated two bleaching steps. Particles in cells expressing WT-K2P3 channels with GFP-SUMO1 or WT-K2P9 channels and GFP-SUMO1 showed only a single bleaching step (n = 100 particles).

NIH-PA Author Manuscript
NIH-PA Author Manuscript
NIH-PA Author Manuscript

NIH-PA Author Manuscript

NIH-PA Author Manuscript

NIH-PA Author Manuscript

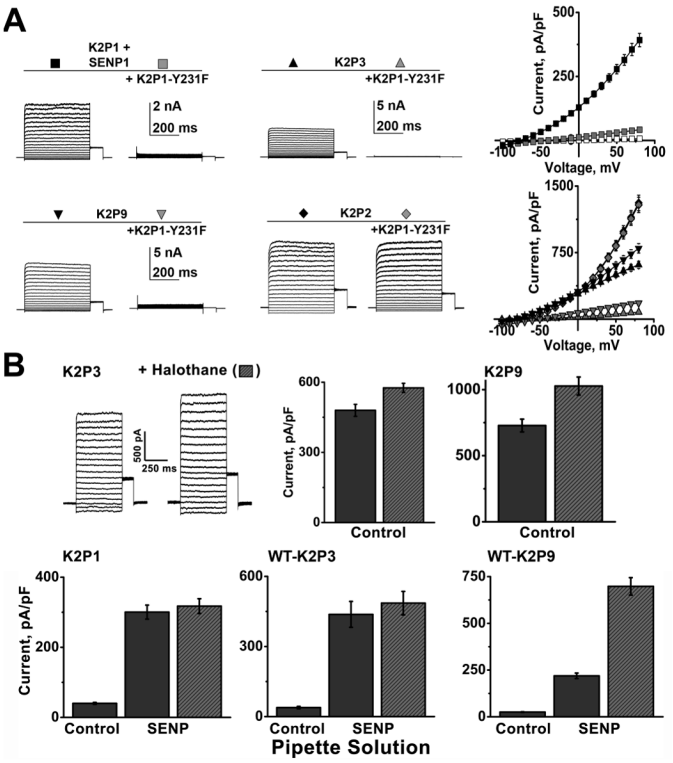

Figure 6. K2P1-Y231F suppression and halothane augmentation of K2P channel activity

Subunits heterologously-expressed in CHO cells were studied in whole-cell mode. Current-voltage relationships and histograms are mean current ± S.E.M. for 8–12 cells per group.

A. Exemplar current families are shown for SENP1-activated K2P1, K2P3, K2P9 and K2P2 expressed without or with (+) K2P1-Y231F. K2P1-Y231F suppressed current passed by K2P1, K2P3 and K2P9 but not K2P2, consistent with assembly of K2P1-Y231F with all but the last subunit type. Current inhibition at 50 mV was 89%, 88% and 76% for SENP1-activated K2P1, K2P3 and K2P9, respectively. Current-voltage relationships are shown; K2P1 basal current is indicated by the open squares.

B. Histograms of current at 50 mV in CHO cells expressing the indicated channels before (solid bars) and on application of halothane (hashed bars). K2P3 and K2P9 were studied with control solution in the pipette. Halothane was applied to K2P1, WT-K2P3 and WT-K2P9 after activation by SENP1 in the pipette; as in patches (Figure 5), these channels pass negligible currents without activation by SENP (control). Halothane augmented channel current in the following order: WT–K2P9 ≫ K2P9 > K2P3 > WT–K2P3 or K2P1.

NIH-PA Author Manuscript

NIH-PA Author Manuscript

NIH-PA Author Manuscript

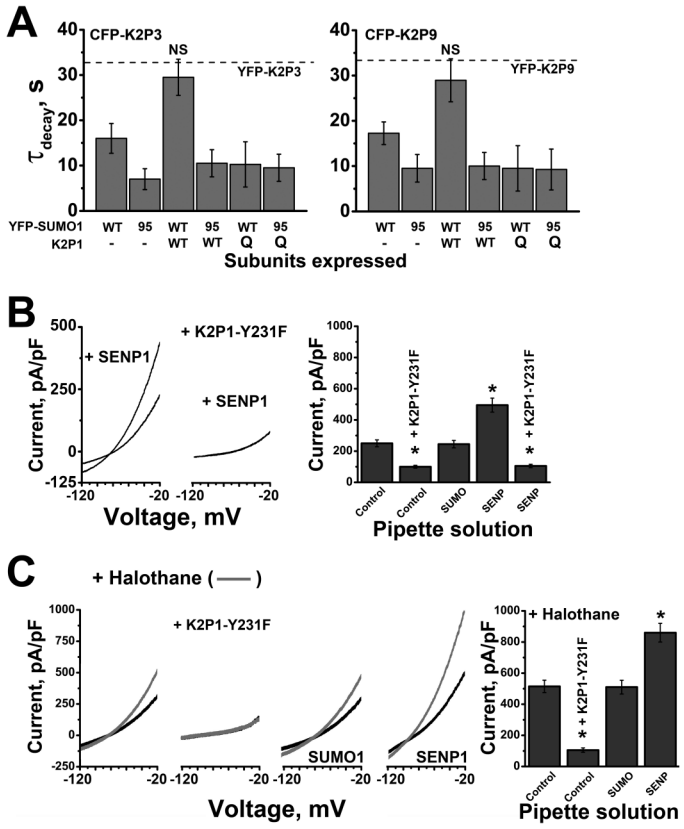

Figure 7. Channels that can incorporate K2P1 mediate the acid-sensitive portion of IKso and are those responsive to halothane

FRET analysis was performed on live CGN that heterologously expressed subunits tagged with CFP or YFP as in Figure 4. Fluorescence decay parameters (mean τ ± S.E.M.) are listed in Table S3. IKso was studied in whole-cell mode, as in Figure 2, with only solution B in the pipette (control), added SUMO1, or added SENP1 (n = 10 cells). Significant changes in IKso magnitude, compared to naive CGN studied with control solution in the pipette, are indicated (*, P<0.001).

A. FRET between CFP-K2P3 (or CFP-K2P9) and YFP-SUMO1 requires K2P1. FRET is observed in homodimeric channels between subunits tagged with CFP and YFP (dotted lines); CFP-K2P3 or CFP-K2P9 show FRET with YFP-SUMO1 when wild type K2P1 (WT) is also expressed (NS, indicates no significant change compared to homodimeric channel FRET signal). Controls: FRET was not observed with heterologous-expression of subunits incapable of sumoylation, YFP-SUMO1$_{95}$ (95) and K2P1-K274Q (Q).

B. Exemplar IKso traces and mean current-density histograms. Left, as shown in Figure 2A (Table S1), SENP1 augments IKso. Middle, heterologous expression of K2P1-Y231F subunits ablates augmentation by SENP1 and diminishes IKso by 60% (to 100 ± 9 pA/pF). SUMO1 does not alter IKso (245 ± 22 pA/pF). In contrast, SENP1 augments IKso by ~200%.

C. Exemplar IKso traces and mean current-density histograms. Application of halothane (gray traces) augments IKso ~200% but has no effect on IKso in cells expressing K2P1-Y231F (105 ± 14 pA/pF). Adding SUMO1 into the pipette does not alter the effect of halothane (510 ± 44 pA/pF). With SENP1 in the pipette, halothane augments IKso ~345% to 860 pA/pF.